# Supplementary Information

## Synergistic boosting electrical output of moisture-electric generator based on CCNF-LiCl-PAM hydrogel

Xinpeng Zhang,[ab] Jiaxuan Liu,[b] Xinyuan Qu,[b] Ao Shen,[b] and Xin Wang *[abc]

[a.]School of Materials and Chemistry, Anhui Agricultural University, Hefei 230036, P. R. China.

[b]Henan Key Laboratory of Quantum Materials and Quantum Energy, School of Future Technology, Henan University, Kaifeng 475004, China.

[c]Anhui Provincial Engineering Center for High-Performance Biobased Nylon, Anhui Agricultural University, Hefei 230036, P. R. China

E-mail: xwang06@ahau.edu.cn and xwang2008@vip.henu.edu.cn

**Movie S3.** 3×1.0 W LED lamps powered by 60 MEG units connected in series.

**Movie S4.** Twelve hygro-thermographs in parallel powered by 12 MEG units connected in parallel.

**Movie S5.** One smartphone directly powered by a 1.0 F capacitor that is charged by the integrated 3×3 MEGs.

**Movie S6.** An LED screen directly powered by a 1.0 F capacitor that is charged by the integrated 3×3 MEGs.

**Movie S7.** Four hygro-thermographs in parallel directly powered by a single 5×5 $cm^2$ CLP-MEG.

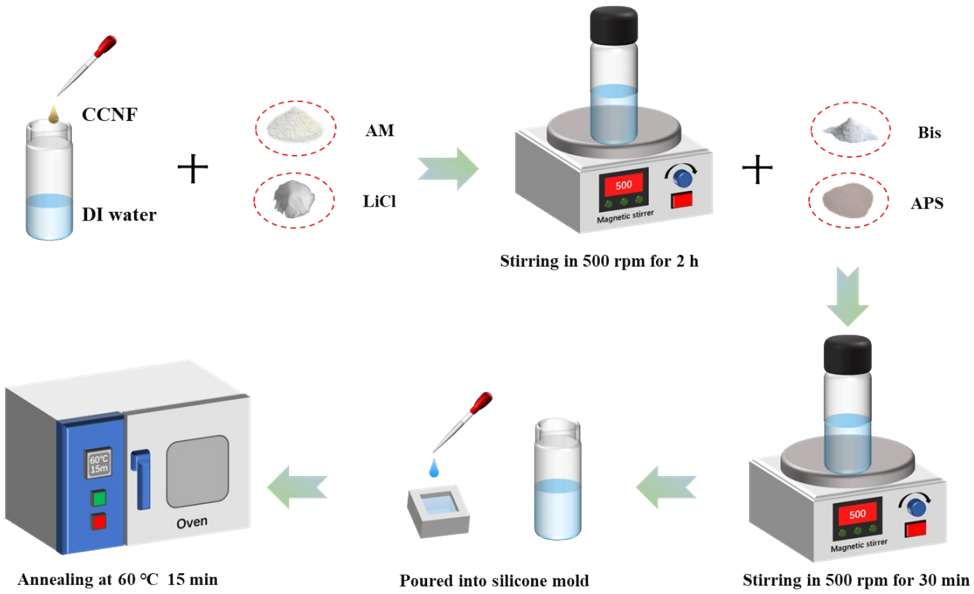


**Fig. S1.** Schematic illustration of preparation process of the CLP hydrogel.

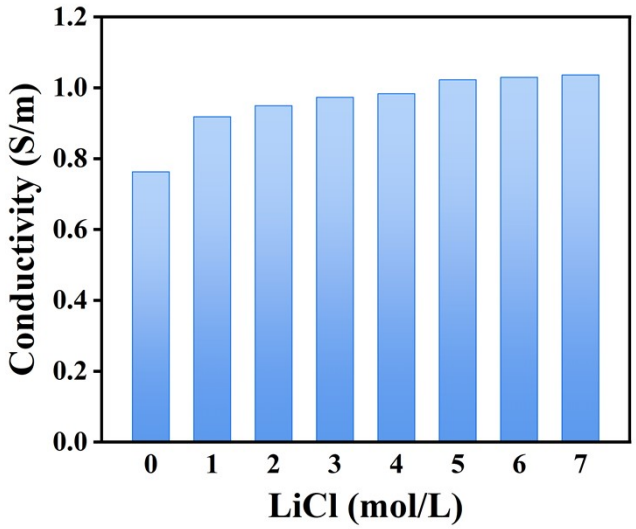


**Fig. S2**. Conductivities of the CLP hydrogels with different LiCl concentrations.

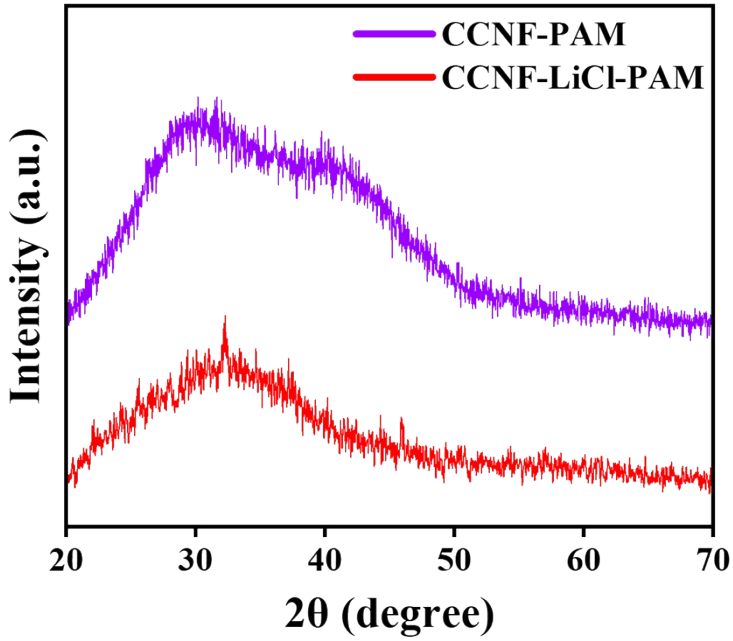


**Fig. S3.** XRD patterns of CCNF-PAM and CCNF-LiCl-PAM (CLP) Hydrogels.

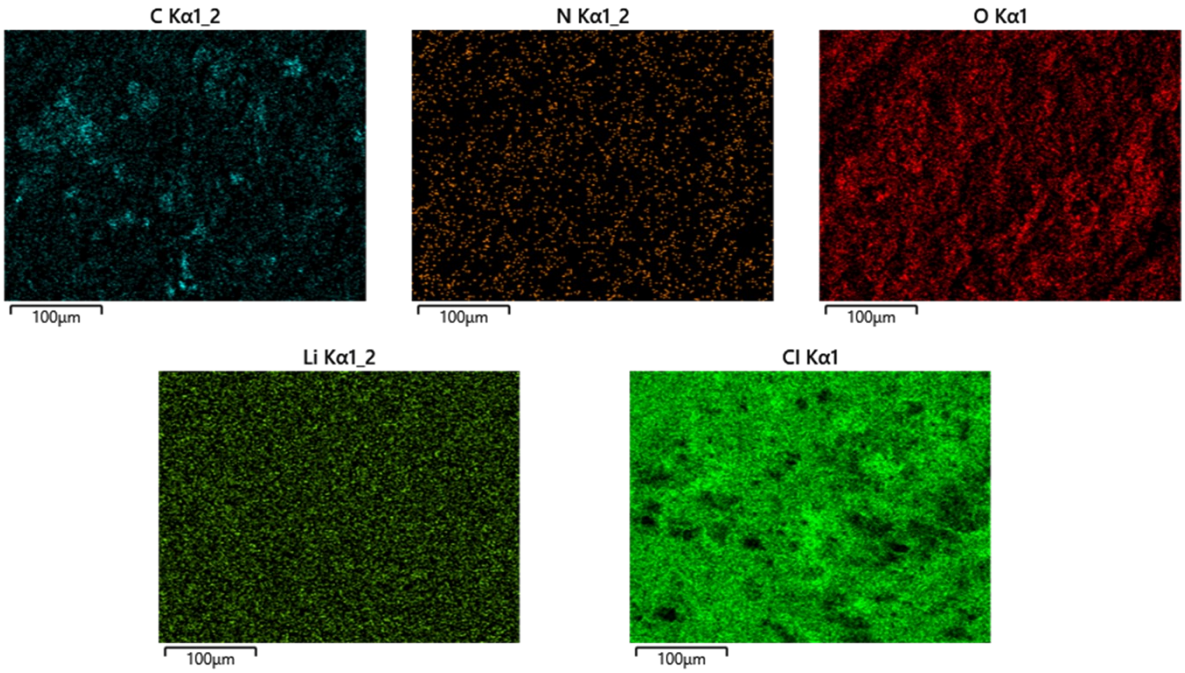


**Fig. S4.** EDS mapping of C, N, O, Li and Cl elements in the CLP hydrogel.

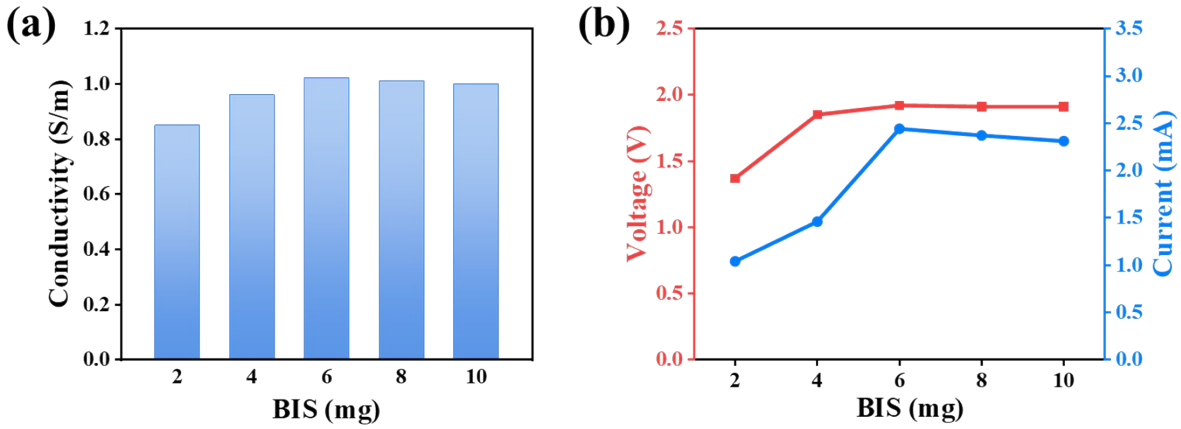


**Fig. S5.** (a) Conductivity of the CLP hydrogel and (b) electrical outputs of the CLP-MEG based on the CLP hydrogel prepared by different BIS contents.

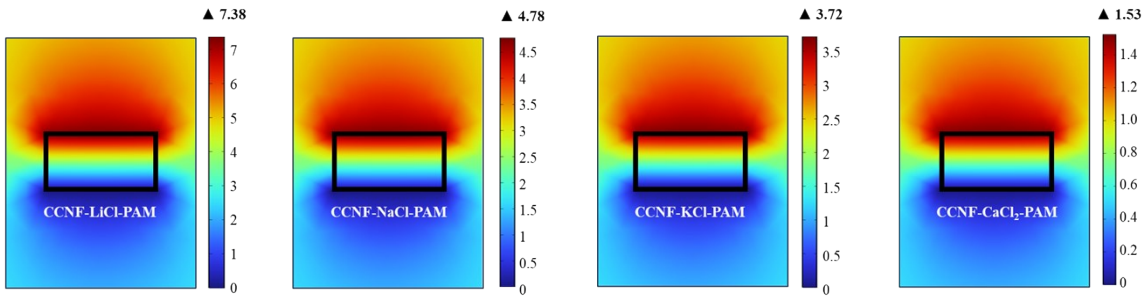


**Fig. S6.** Surface potentials of MEGs with different salts were simulated using COMSOL software. The highest and lowest surface potential belongs to the MEGs with monovalent $Li^{+}$ and divalent $Ca^{2+}$ ions, respectively. Under the same conditions, the greater difference in surface potential of the nanochannels, the faster the ions migration within the channels.

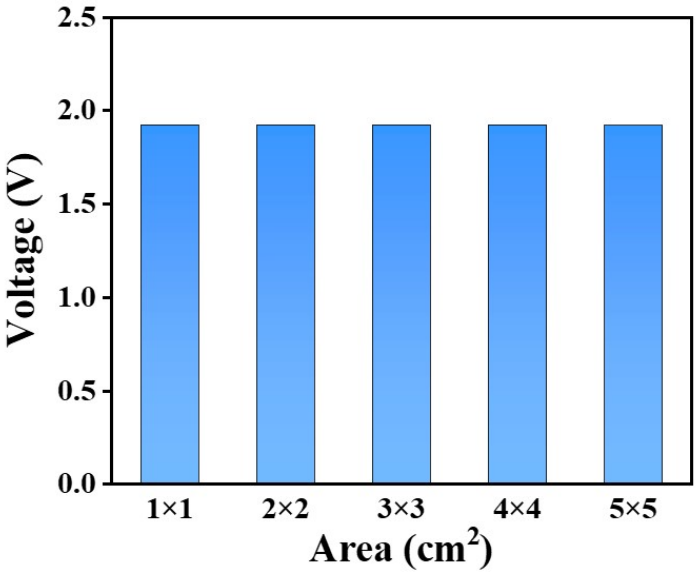


**Fig. S7.** Output voltages of the CLP-MEGs with different areas.

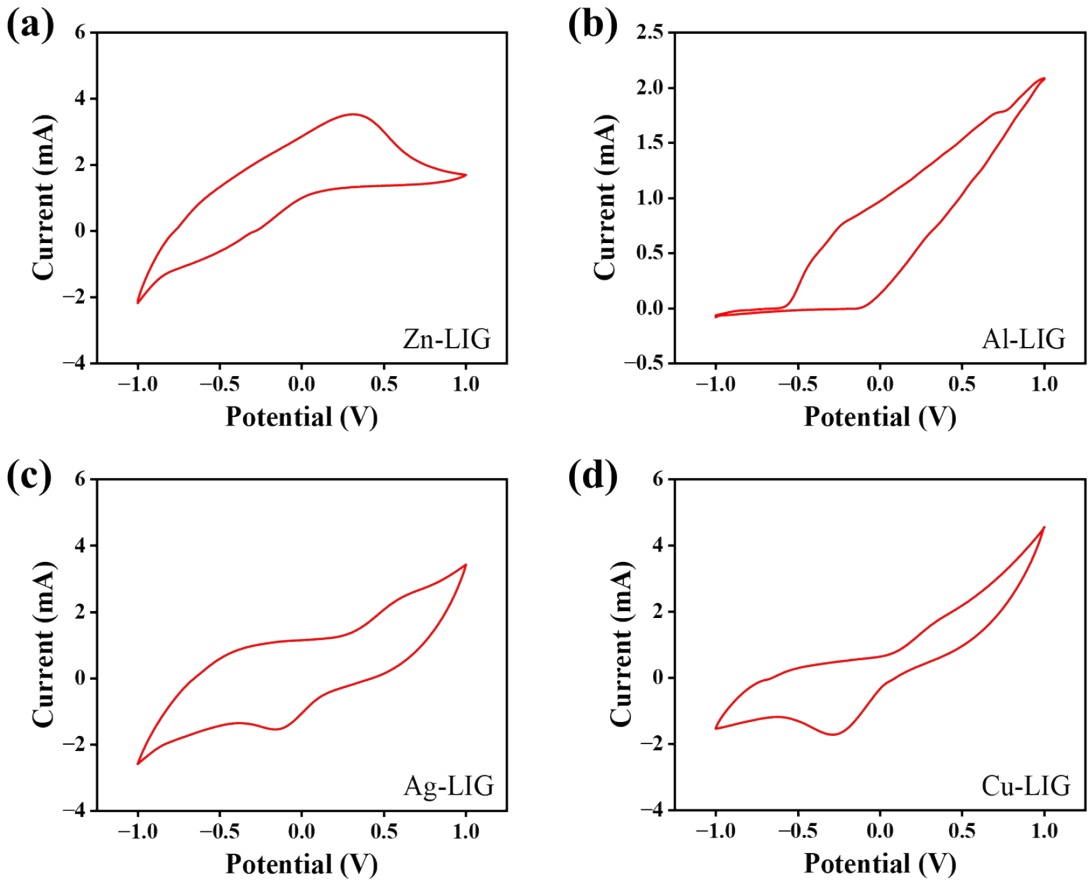


**Fig. S8.** CV curves of the CLP-MEG with different top electrodes (Zn, Al, Ag, and Cu).

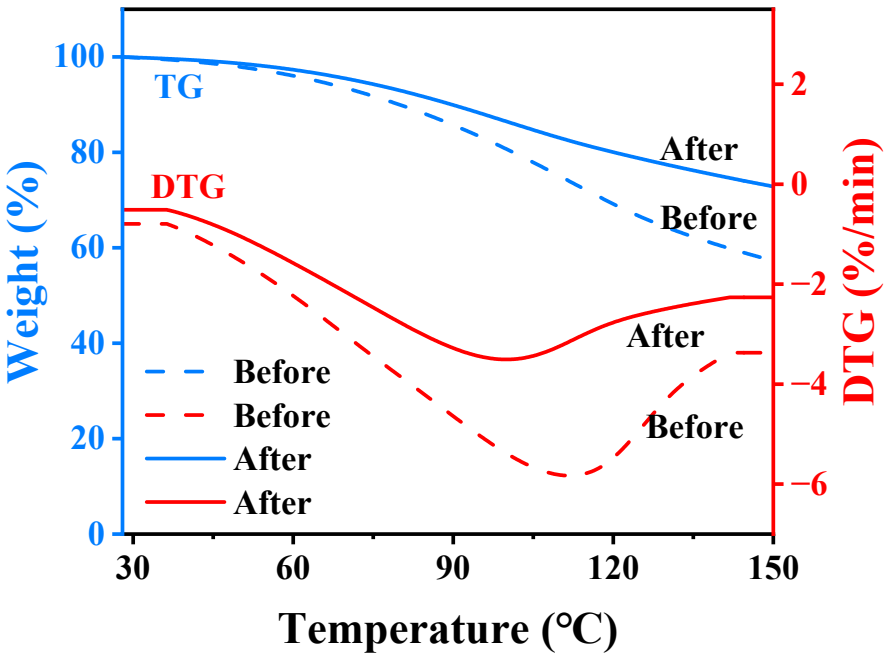


**Fig. S9.** TG and DTG curves of the pristine CLP hydrogel and the CLP hydrogel after 90 days.

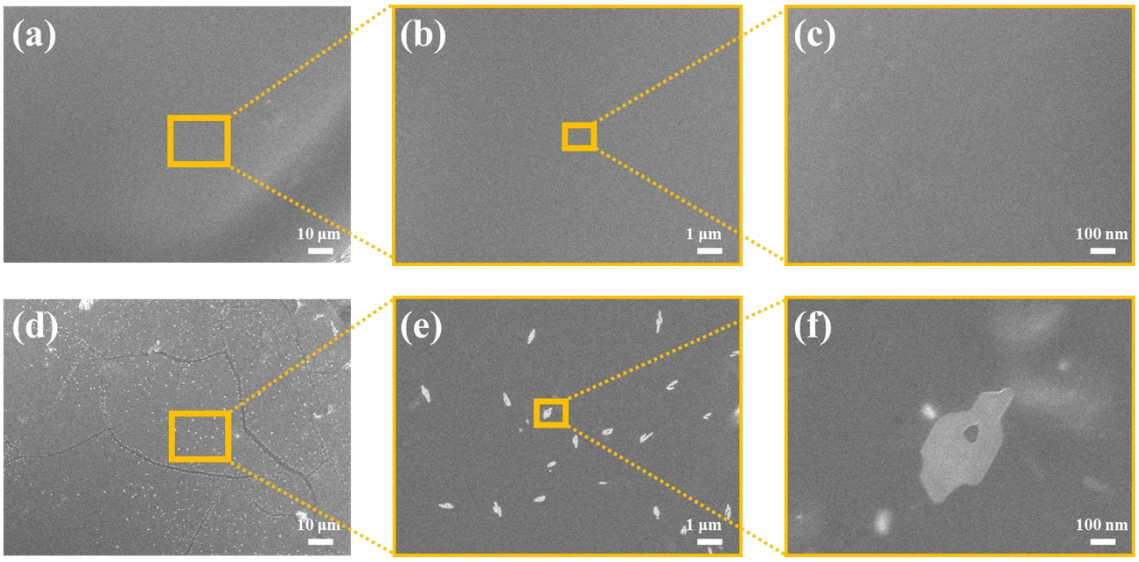


**Fig. S10.** SEM images of the pristine Zn electrode (a-c) and the Zn electrode after 90 days (d-f).

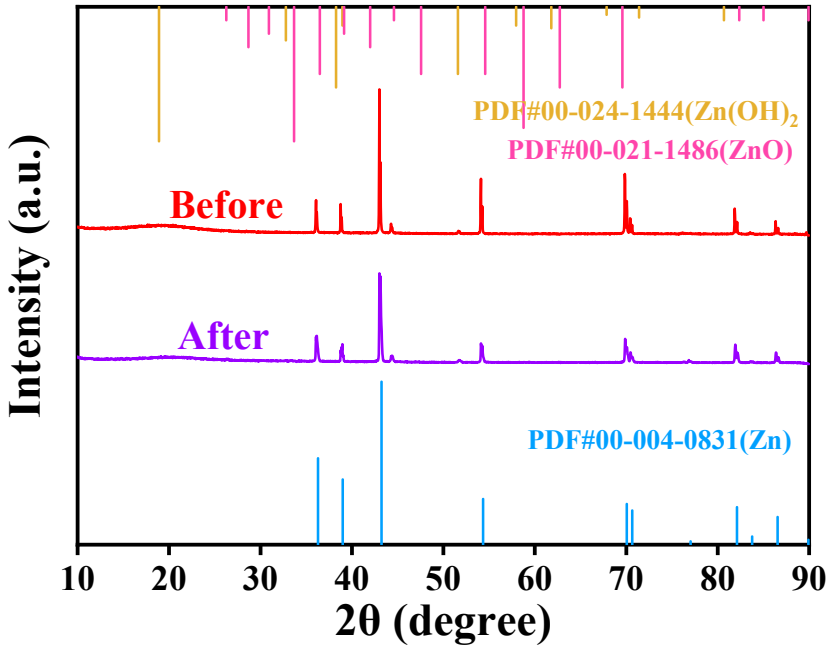


**Fig. S11.** XRD patterns of the pristine Zn electrode and the Zn electrode after 90 days.

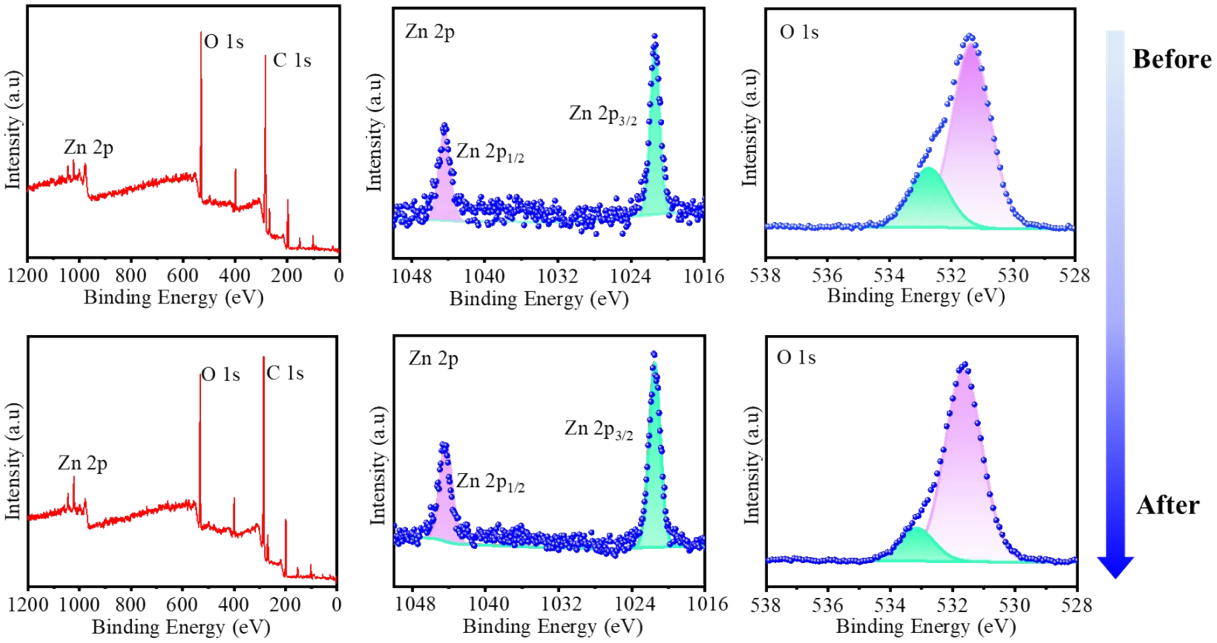


**Fig. S12.** XPS spectra of the Zn electrode before and after 90 days.

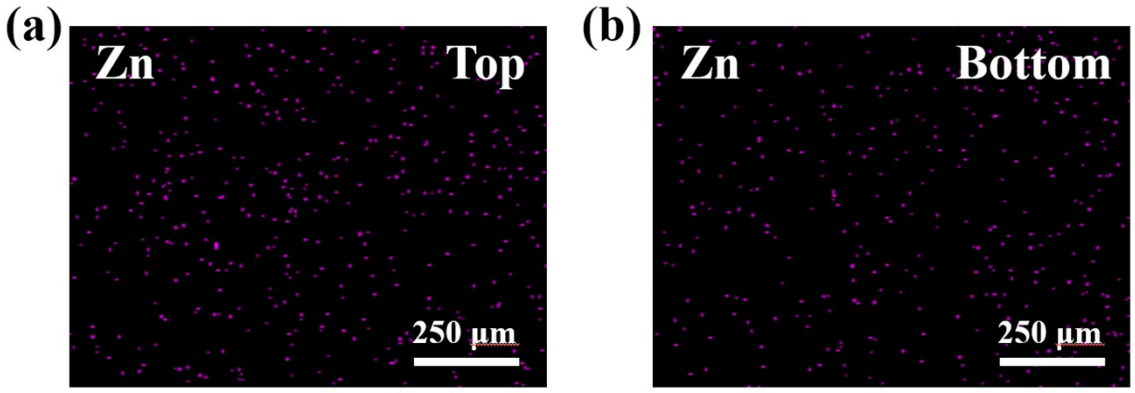


**Fig. S13.** EDS mapping of Zn element on top and bottom surfaces of the CLP hydrogel after 90 days.

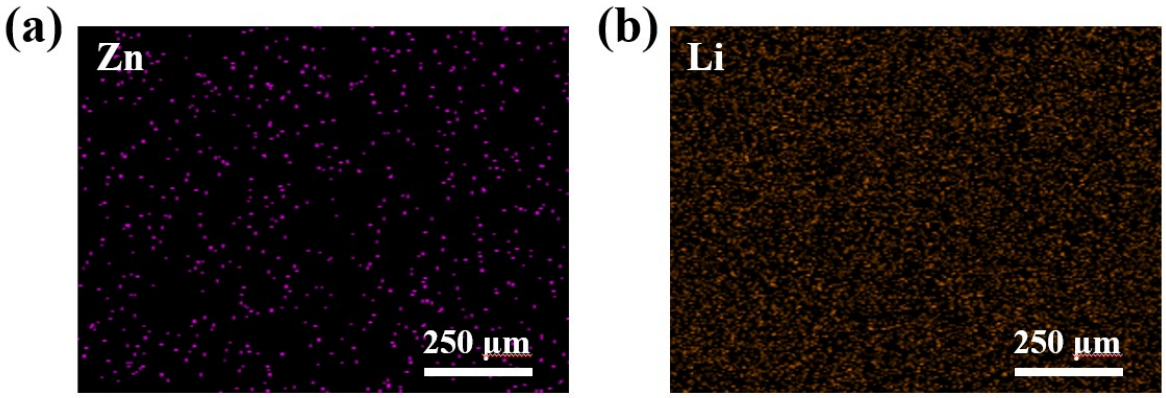


**Fig. S14.** EDS mapping of Zn and Li elements on the LIG electrode after 90 days.

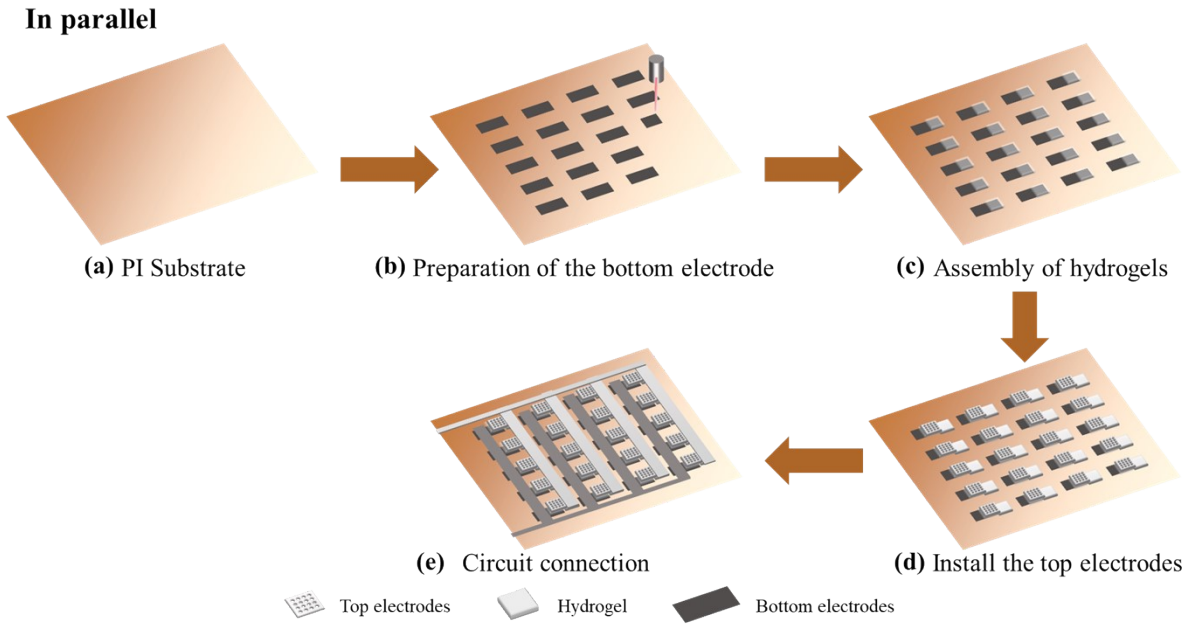


**Fig. S15.** Schematic illustration of fabrication process of the parallel-integrated MEGs. (a) PI substrate. (b) Fabrication of LIG electrodes on the PI substrate using a programmable laser engraving machine. (c) Assembly of the prepared hydrogel onto the bottom LIG electrode. (d) Assembly of top porous-Zn electrodes on the hydrogel surface. (e) The parallel-integrated MEGs are fabricated via end-to-end and head-to-head connections.

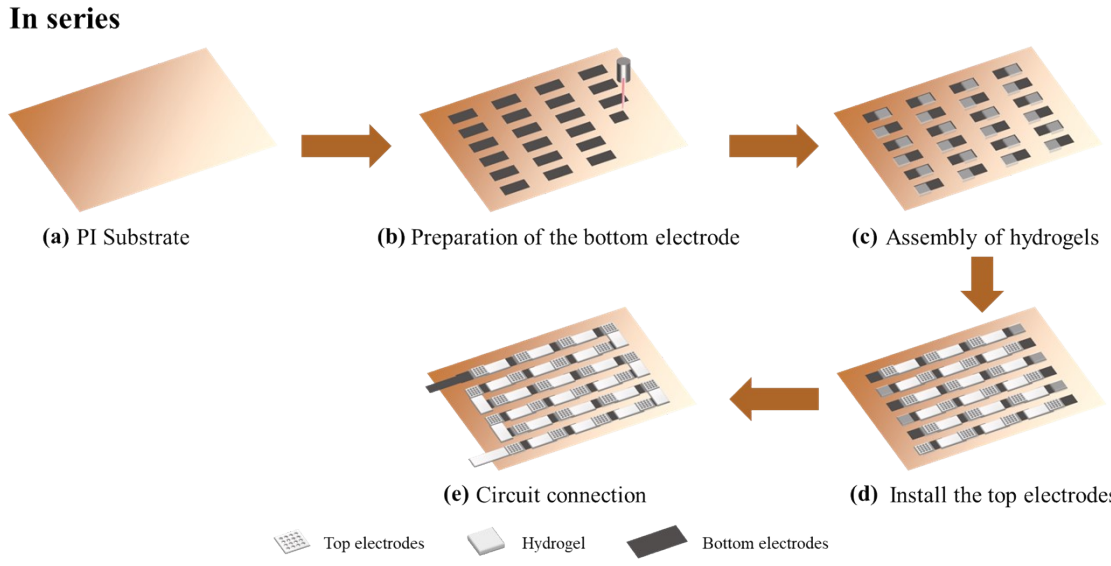


**Fig. S16.** Schematic illustration of fabrication process of the series-integrated MEGs. (a) PI substrate. (b) Fabrication of LIG electrodes on the PI substrate using a programmable laser engraving machine. (c) Assembly of the prepared hydrogel onto the bottom LIG electrode. (d) Assembly of top porous-Zn electrodes on the hydrogel surface. (e) The series-integrated MEGs are fabricated via head-to-end connections.

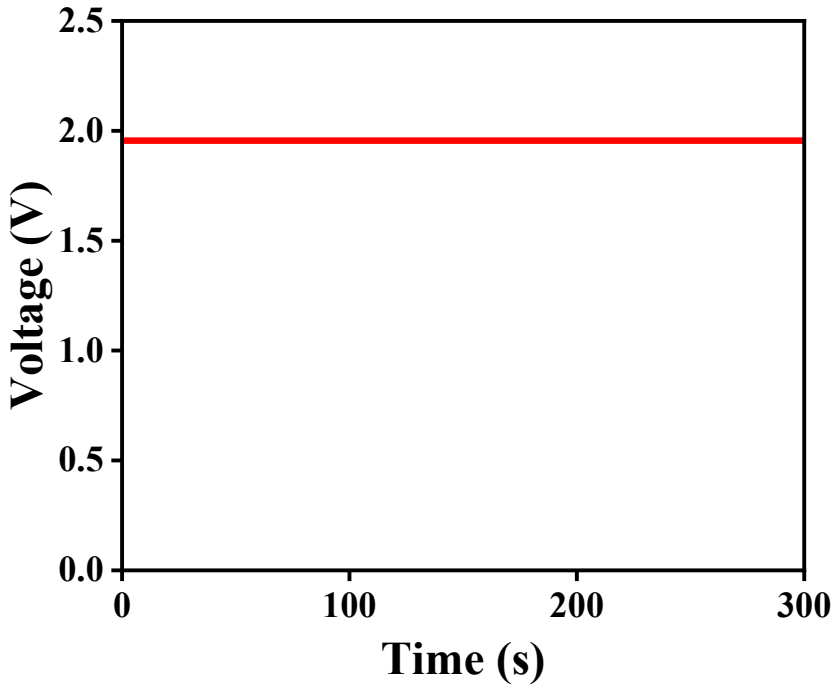


**Fig. S17.** Voltage output of 90 MEG units connected in parallel.

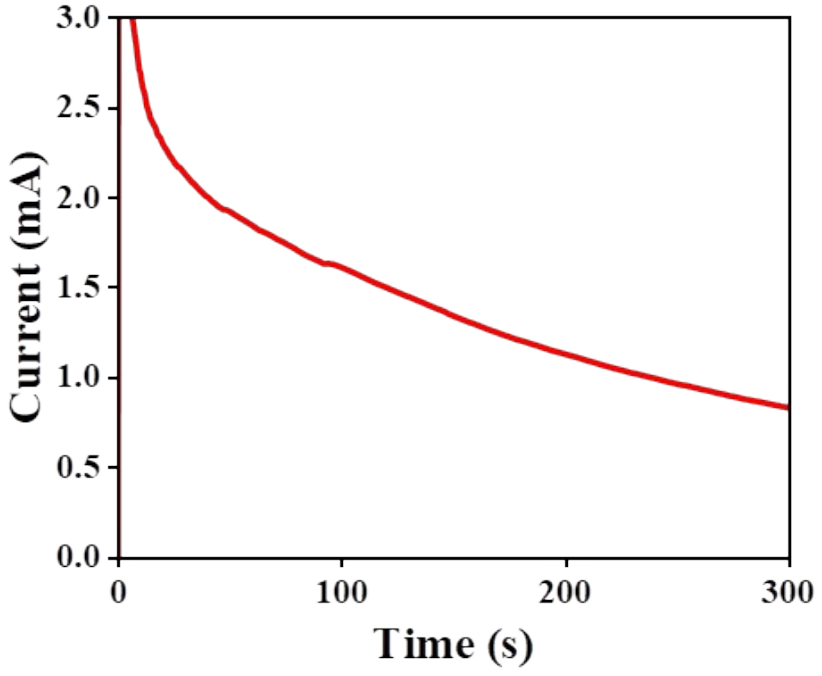


**Fig. S18.** Current output of 60 MEG units connected in series.

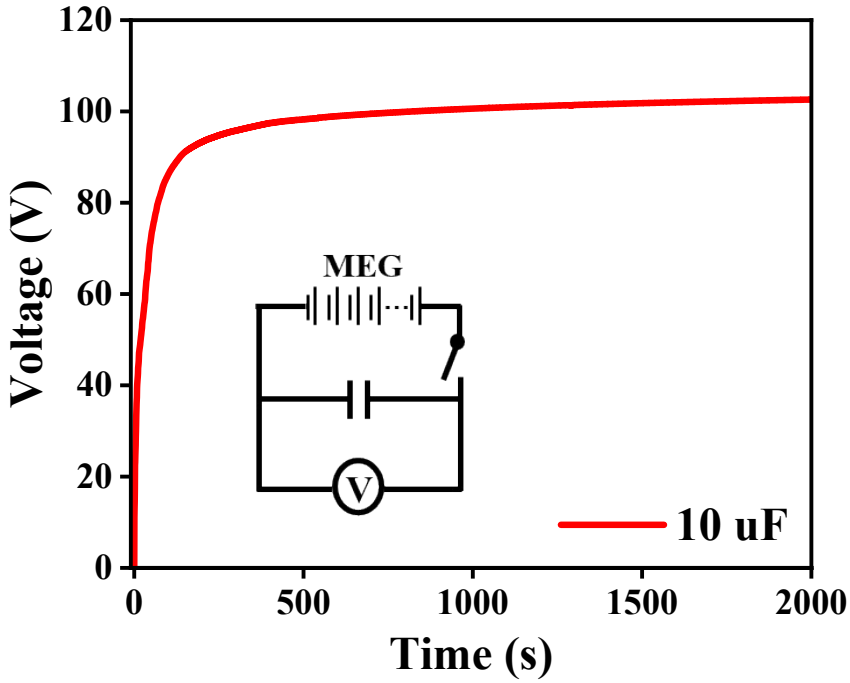


**Fig. S19.** Voltage curve of a 10 μF commercial capacitor charged directly by 60 MEG units connected in series. The inset shows the corresponding circuit diagram.

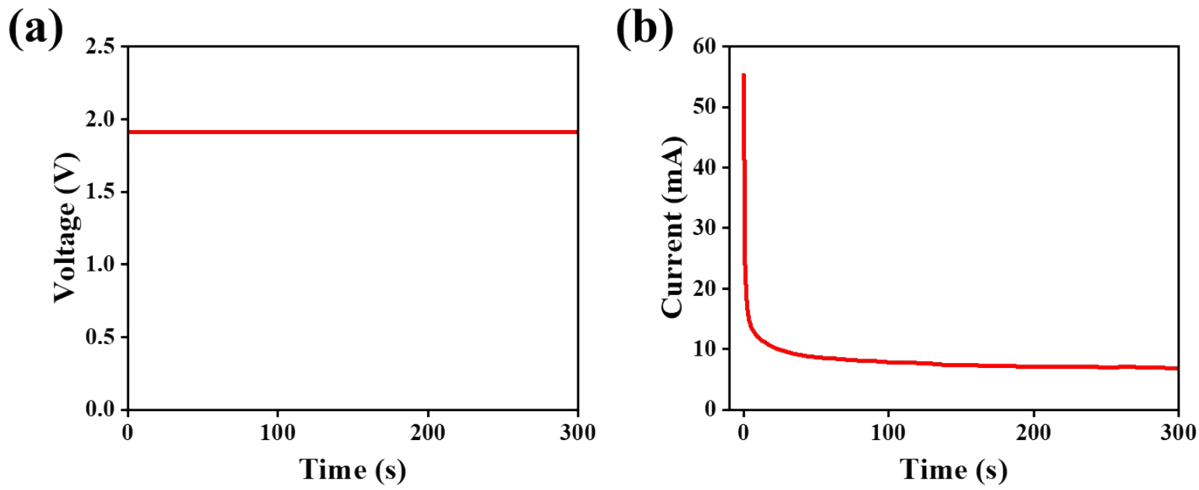


**Fig. S20.** Output voltage (a) and current (b) of 12 MEG units connected in parallel.

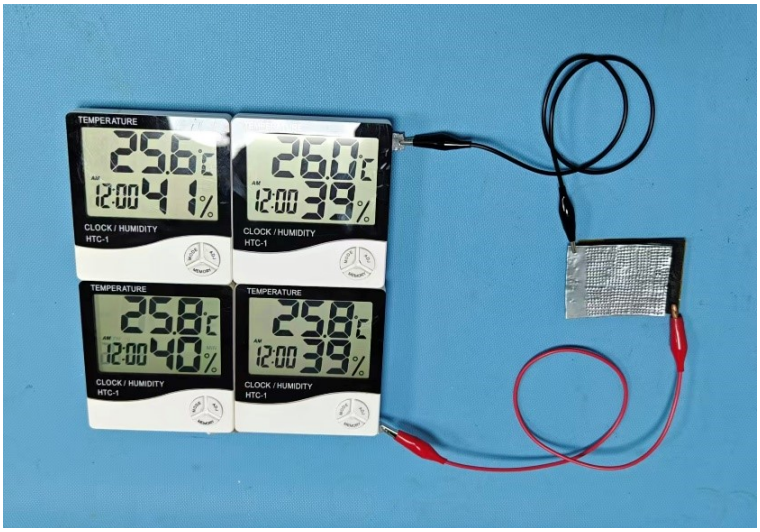


**Fig. S21.** Photography of four hygro-thermographs in parallel directly powered by a single large-area CLP-MEG (5×5 $cm^2$).

**Table S1.** EDS elemental composition on top surface of the CLP hydrogel after 90 days.

| Element | Line Type | Weight Percentage (%) | Wt % Sigma | Atomic Percentage (%) |
|---|---|---|---|---|
| C | K series | 48.47 | 0.73 | 56.97 |
| O | K series | 35.71 | 0.61 | 31.51 |
| Cl | K series | 6.81 | 0.13 | 2.71 |
| N | K series | 8.68 | 1.01 | 8.74 |
| Zn | K series | 0.34 | 0.13 | 0.07 |
| **Total** | | **100.00** | | **100.00** |

**Table S2.** EDS elemental composition on bottom surface of the CLP hydrogel after 90 days.

| Element | Line Type | Weight Percentage (%) | Wt % Sigma | Atomic Percentage (%) |
|---|---|---|---|---|
| C | K series | 47.81 | 0.75 | 56.09 |
| O | K series | 35.86 | 0.64 | 31.58 |
| Cl | K series | 6.61 | 0.13 | 2.63 |
| N | K series | 9.62 | 1.06 | 9.68 |
| Zn | K series | 0.09 | 0.13 | 0.02 |
| **Total** | | **100.00** | | **100.00** |